

## Article

# Effect of the Solvent on the Crystallographic and Magnetic Properties of Rhenium(IV) Complexes Based on 2,2'-Bipyrimidine Ligand

Adrián Sanchis-Perucho, Marta Orts-Arroyo, Nicolas Moliner and José Martínez-Lillo \* 

Departament de Química Inorgànica/Institut de Ciència Molecular (ICMol), Universitat de València, c/Catedrático José Beltrán 2, Paterna, 46980 València, Spain

\* Correspondence: f.jose.martinez@uv.es; Tel.: +34-9635-44460

**Abstract:** Two solvated rhenium(IV) complexes with formula  $[\text{ReCl}_4(\text{bpym})]\cdot\text{MeCN}$  (**1**) and  $[\text{ReCl}_4(\text{bpym})]\cdot\text{CH}_3\text{COOH}\cdot\text{H}_2\text{O}$  (**2**) (bpym = 2,2'-bipyrimidine) have been prepared and characterized by means of Fourier transform infrared spectroscopy (FT-IR), scanning electron microscopy and energy dispersive X-ray analysis (SEM-EDX), single-crystal X-ray diffraction (XRD) and SQUID magnetometer. **1** and **2** crystallize in the monoclinic system with space groups  $P2_1/n$  and  $P2_1/c$ , respectively. In both compounds, the Re(IV) ion is six-coordinate and bound to four chloride ions and two nitrogen atoms of a 2,2'-bipyrimidine molecule forming a distorted octahedral geometry around the metal ion. In the crystal packing of **1** and **2**, intermolecular halogen...halogen and  $\pi$ ...halogen-type interactions are present. Hydrogen bonds take place only in the crystal structure of **2**. Both compounds exhibit a similar crystal framework based on halogen bonds. Variable temperature dc magnetic susceptibility measurements performed on microcrystalline samples of **1** and **2** show a similar magnetic behavior for both compounds, with antiferromagnetic exchange between the Re(IV) ions connected mainly through intermolecular Re-Cl...Cl-Re interactions.

**Keywords:** rhenium; 2,2'-bipyrimidine; metal complexes; crystal structure; crystal explorer; magnetic properties



**Citation:** Sanchis-Perucho, A.; Orts-Arroyo, M.; Moliner, N.; Martínez-Lillo, J. Effect of the Solvent on the Crystallographic and Magnetic Properties of Rhenium(IV) Complexes Based on 2,2'-Bipyrimidine Ligand. *Inorganics* **2023**, *11*, 78. <https://doi.org/10.3390/inorganics11020078>

Academic Editors: Duncan H. Gregory, Wolfgang Linert, Richard Dronskowski, Vladimir Arion, Claudio Pettinari and Torben R. Jensen

Received: 29 December 2022

Revised: 1 February 2023

Accepted: 6 February 2023

Published: 9 February 2023



**Copyright:** © 2023 by the authors. Licensee MDPI, Basel, Switzerland. This article is an open access article distributed under the terms and conditions of the Creative Commons Attribution (CC BY) license (<https://creativecommons.org/licenses/by/4.0/>).

## 1. Introduction

The study of solvate formation in crystalline compounds is becoming an increasingly significant topic given the academic and industrial interest in elucidating the properties and variations in the morphology of different crystal forms [1,2]. In many cases, the crystallization solvent can explain the observed changes in physical properties of a crystalline material, and this investigation can assist in the ongoing efforts to improve the design of crystallization processes from solution [1–5].

In the coordination chemistry of Re(IV) (a  $5d^3$  ion), the polymorphism and the effect of the solvent on the magnetic properties of Re(IV) complexes have been relatively little studied [6,7]. The mononuclear complexes based on halides of Re(IV) ion have been investigated during the past few decades and are characterized by large values of magnetic anisotropy and significant intermolecular magnetic exchange [8–22]. Indeed, these compounds can display relatively strong dipolar exchange through Re-X...X-Re type contacts (X = halogen), which can result in a magnetic order as, for instance, metamagnetism or spin-canting phenomenon [23–25]. Such studies have also revealed the occurrence of significant antiferromagnetic interactions between the paramagnetic Re(IV) metal ions [Re(IV) has three unpaired electrons and a  $^4A_{2g}$  term as ground electronic state]. These interactions are not transmitted across a chemical bond but through the aforementioned intermolecular contacts. These exchange pathways are supported by DFT-type calculations on the mononuclear Re(IV) complexes, which showed that spin density from the metal ion is somewhat delocalized onto the peripheral atoms of the ligands [7]. Given

that the intermolecular halogen···halogen distance depends on the countercation size, bulky cations such as tetraphenylarsonium ( $\text{AsPh}_4^+$ ) and tetra-*n*-butylammonium ( $\text{NBu}_4^+$ ) preclude the magnetic coupling between adjacent halides of Re(IV) ions due to the large X···X separation they generate [7]. In singular cases, an unusual Re–Cl···(H<sub>2</sub>O)···Cl–Re pathway leads these Re(IV) compounds to ferromagnetic interactions. Hence, this halogen···halogen separation can also be affected by solvent molecules. As such, the use of adequate solvents could provide deeper insights into the magnetic properties of these types of Re(IV) systems.

The neutral mononuclear  $[\text{ReCl}_4(\text{bpym})]$  complex has been previously investigated, showing remarkable properties [26]. It displays potent *in vitro* anti-proliferative activity against a series of cancer cells [27]. Regarding its magnetic properties, it exhibits magnetic ordering below 7.0 K through the spin-canting phenomenon, with coercive field (H<sub>c</sub>) and remanent magnetization (M<sub>r</sub>) values of 1750 G and 0.05 μ<sub>B</sub>, respectively [28]. It has also been employed as a starting material for the preparation of rhenium-based compounds such as, for instance, the first heterodinuclear 2,2'-bipyrimidine-bridged complex magneto-structurally studied, in the formula  $[\text{ReCl}_4(\mu\text{-bpym})\text{NiBr}_2(\text{H}_2\text{O})_2]$  [29], and in the chiral, photoluminescent and spin-canted compound of formula  $\{\text{CuReCl}_4(\mu\text{-Cl})(\mu\text{-pyz})[\text{ReCl}_4(\mu\text{-bpym})]\}\cdot\text{MeNO}_2$  [30]. More recently, two one-dimensional coordination polymers of general formula  $\{[\text{ReCl}_4(\mu\text{-bpym})\text{CuX}_2]\cdot\text{solvent}\}_n$  have been characterized structurally and magnetically [31].

To develop our investigation on the effect of the solvent and the intermolecular interactions on the magnetic properties of Re(IV) compounds, we herein report the synthesis, crystal structure and magnetic properties of two solvated Re(IV) complexes based on the 2,2'-bipyrimidine ligand, with formula  $[\text{ReCl}_4(\text{bpym})]\cdot\text{MeCN}$  (**1**) and  $[\text{ReCl}_4(\text{bpym})]\cdot\text{CH}_3\text{COOH}\cdot\text{H}_2\text{O}$  (**2**), whose properties are compared with those of the non-solvated complex.

## 2. Results and Discussion

### 2.1. Preparation of the Complexes

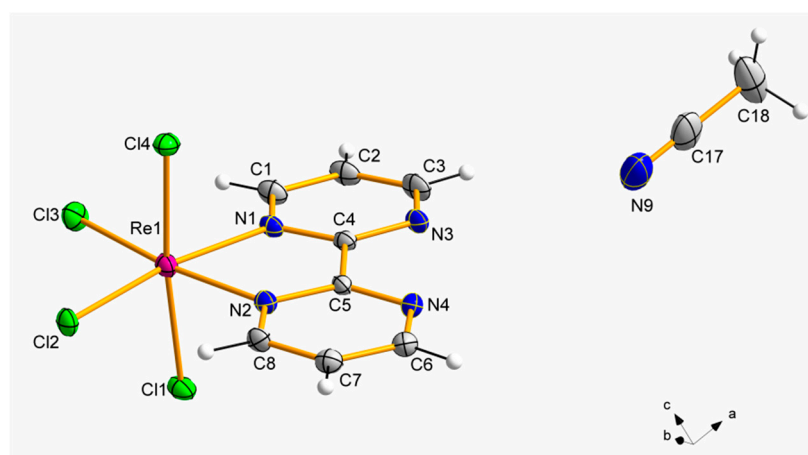
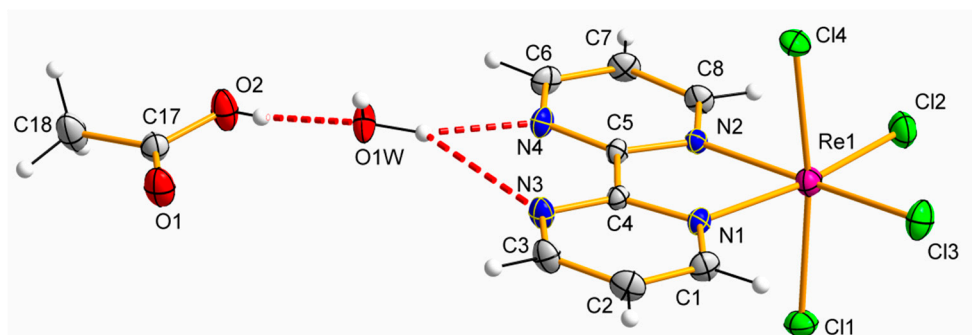
Ammonium hexachlororhenate and 2,2'-bipyrimidine (bpym) were stirred in *N,N*-dimethylformamide (DMF) for 4 h at 110 °C. After cooling, the dark brown solution was filtered and evaporated at 60 °C until the elimination of the solvent was complete. The brown residue was washed with acidified H<sub>2</sub>O and left to air dry. This solid was then shaken with dichloromethane for 30 min and the resulting solution was filtered. The insoluble residue was discarded. The filtrate was washed several times with portions of H<sub>2</sub>O in a separation funnel until the aqueous layer became almost colorless. The dark orange dichloromethane layer was then dried and the solvent evaporated under reduced pressure to leave an orange–yellow microcrystalline solid which was finally dried at 110 °C. The same compound can be obtained from the tetrabutylammonium salt instead of the ammonium salt in acetic acid. Compound **1** was obtained via the recrystallization in a *N,N*-dimethylformamide-acetonitrile mixture, followed by slow diffusion in isopropanol at room temperature. Compound **2** was prepared by means of ligand substitution reaction, by replacing the oxalate (ox) ligand by 2,2'-bipyrimidine in the  $[\text{ReCl}_4(\text{ox})]^{2-}$  complex in a mixture based on acetic acid, which was heated to 100 °C and stirred for 4 h.

### 2.2. Description of the Crystal Structures

The crystal structures of **1** and **2** were studied through the single-crystal X-ray diffraction technique. Both compounds crystallized in the monoclinic crystal system with space groups  $P2_1/n$  and  $P2_1/c$ , respectively (Table 1). The non-solvated  $[\text{ReCl}_4(\text{bpym})]$  complex crystallizes in the orthorhombic space group  $P2_12_12_1$  [26]. The crystal structure of **1** is made up of neutral  $[\text{ReCl}_4(\text{bpym})]$  complexes and MeCN molecules, whereas the crystal structure of **2** is based on  $[\text{ReCl}_4(\text{bpym})]$ , CH<sub>3</sub>COOH and H<sub>2</sub>O molecules, as shown in their respective asymmetric units (Figures 1 and 2).

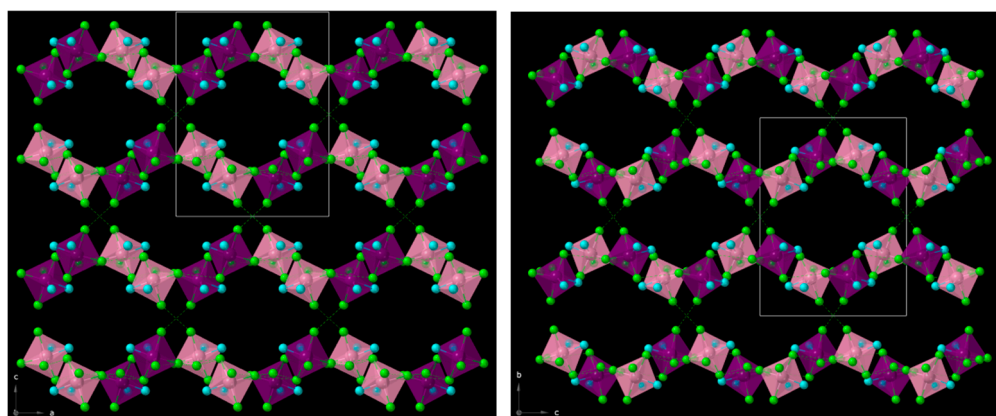
**Table 1.** Summary of the crystal data and structure refinement parameters for **1** and **2**.

Compound	1	2
CIF	2,233,243	2,233,244
Formula	C <sub>18</sub> H <sub>15</sub> Cl <sub>8</sub> N <sub>9</sub> Re <sub>2</sub>	C <sub>18</sub> H <sub>18</sub> Cl <sub>8</sub> N <sub>8</sub> O <sub>3</sub> Re <sub>2</sub>
Fw/g mol <sup>-1</sup>	1013.39	1050.40
Temperature/K	120(2)	120(2)
Crystal system	monoclinic	monoclinic
Space group	<i>P</i> 2 <sub>1</sub> / <i>n</i>	<i>P</i> 2 <sub>1</sub> / <i>c</i>
<i>a</i> /Å	13.239(1)	11.960(1)
<i>b</i> /Å	11.852(1)	18.089(1)
<i>c</i> /Å	17.666(1)	13.433(1)
$\alpha$ /°	90	90
$\beta$ /°	90.02(1)	93.02(1)
$\gamma$ /°	90	90
<i>V</i> /Å <sup>3</sup>	2771.97(13)	2902.30(10)
<i>Z</i>	4	4
<i>D</i> <sub>c</sub> /g cm <sup>-3</sup>	2.428	2.404
$\mu$ (Mo-K $\alpha$ )/mm <sup>-1</sup>	9.526	9.110
<i>F</i> (000)	1888	1968
Goodness-of-fit on <i>F</i> <sup>2</sup>	1.307	1.061
<i>R</i> <sub>1</sub> [ <i>I</i> > 2 $\sigma$ ( <i>I</i> )]/all data	0.0221/0.0252	0.0377/0.0424
<i>wR</i> <sub>2</sub> [ <i>I</i> > 2 $\sigma$ ( <i>I</i> )]/all data	0.0649/0.0773	0.0793/0.0816

**Figure 1.** Detail of the mononuclear [ReCl<sub>4</sub>(bpym)] complex and solvent MeCN molecule in **1**. Thermal ellipsoids are depicted at the 50% probability level.**Figure 2.** Detail of the mononuclear [ReCl<sub>4</sub>(bpym)] complex and solvent molecules in **2**. Thermal ellipsoids are depicted at the 50% probability level. H-bonding interactions are highlighted as dashed lines.

In the mononuclear  $[\text{ReCl}_4(\text{bpym})]$  complexes of **1** and **2**, each Re(IV) ion is bonded to four chloride ions and two nitrogen atoms of a 2,2'-bipyrimidine molecule, forming a distorted octahedral geometry around the metal ion. In both compounds, the average values of the Re–N bond lengths [2.129(1) Å for **1** and 2.137(1) Å for **2**] are shorter than those of the Re–Cl bond lengths [2.317(1) Å for **1** and 2.308(1) Å for **2**], displaying values which are in agreement with those previously published for similar Re(IV) complexes [26,32]. It is worth noting that the Re–Cl bond lengths in axial positions are longer than those located in equatorial positions in both **1** and **2** (Figures 1 and 2). The chelating 2,2'-bipyrimidine molecule is effectively planar in both compounds. However, in the non-solvated complex, the two pyrimidine rings show a tilted position with a dihedral angle between them of ca.  $16.0(3)^\circ$  [26]. In **1** and **2**, the 2,2'-bipyrimidine ligand exhibits average C–C, N–N, and C–N bond length values in agreement with those found in similar bpym-based complexes containing 4d and 5d metal ions [33,34].

In the crystal packing of **1**, intermolecular short Cl $\cdots$ Cl contacts of 3.559(1) Å [Cl(3) $\cdots$ Cl(7a) distance with (a) =  $x - 1, y, z$ ] and 3.560(1) Å [Cl(2) $\cdots$ Cl(6b) distance with (b) =  $x - 1, y - 1, z$ ] direct alternate chains formed by complexes of Re(1) and Re(2) ions, which grow along the crystallographic *c* axis (Figure 3). These chains are interlinked through C–H $\cdots$ N interactions involving neighboring bpym ligands [C(15c) $\cdots$ N(4) distance being ca. 3.50 Å; (c) =  $x, y - 1, z$ ], and also with somewhat longer Cl $\cdots$ Cl contacts of ca. 3.667(1) Å, resulting in a corrugated layered structure that grows in the *ac* plane (Figure 3). Further C–H $\cdots$ N interactions [C(6d) $\cdots$ N(9) distance being ca. 3.62 Å; (d) =  $-x + 1, -y + 2, -z + 1$ ] occur between  $[\text{ReCl}_4(\text{bpym})]$  complexes and MeCN solvent molecules.  $\pi\cdots\text{Cl}$  contacts of ca. 3.283(1) Å can be considered halogen bonds, which, along with several weak C–H $\cdots$ Cl interactions, draw together a 3D crystal structure in compound **1**.

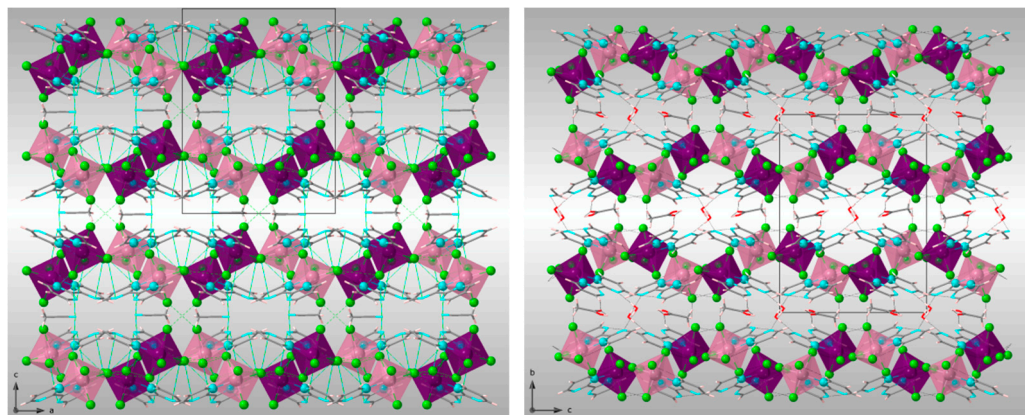


**Figure 3.** View along the crystallographic *b* axis of the one-dimensional motifs of  $[\text{ReCl}_4(\text{bpym})]$  complexes (polyhedron model) connected through Cl $\cdots$ Cl interactions in **1** (left); View along the crystallographic *a* axis of the one-dimensional motifs of  $[\text{ReCl}_4(\text{bpym})]$  complexes (polyhedron model) connected through Cl $\cdots$ Cl interactions in **2** (right). Solvent molecules and bpym ligand have been omitted for clarity.

In the crystal packing of **2**, several O–H $\cdots$ O and O–H $\cdots$ N hydrogen bonds connect the solvent molecules  $\text{CH}_3\text{COOH}$  and  $\text{H}_2\text{O}$  to the  $[\text{ReCl}_4(\text{bpym})]$  complexes [O1w $\cdots$ N(7a) distance of ca. 2.866 Å; (a) =  $-x + 1, y - 1/2, -z + 3/2$ ] (Table 2). As in **1**, chains formed through alternate complexes of Re(1) and Re(2) ions are generated by very short Cl $\cdots$ Cl contacts (Figure 3). In the case of **2**, these types of halogen $\cdots$ halogen bonds are shorter than those found in **1** [the shortest one being Cl(3) $\cdots$ Cl(7b) with a distance of ca. 3.309 Å and (b) =  $x + 1, -y + 3/2, z + 1/2$ ] (Figure 3). Further Cl $\cdots$ Cl contacts of approximately 3.708 Å, together with C–H $\cdots$ N interactions between bipyrimidine rings of adjacent  $[\text{ReCl}_4(\text{bpym})]$  complexes, link the chains forming 2D sheets [C(6c) $\cdots$ N(8) distance of ca. 3.507 Å; (c) =  $x, -y + 3/2, z + 1/2$ ] (Figure 4).

**Table 2.** Selected hydrogen-bonding interactions in **2**.

D-H...A	D-H/Å	H...A/Å	D...A/Å	(DHA) <sup>o</sup>
O(1w)-H(1wB)...N(4)	0.927	1.91(1)	2.804(1)	162.7(1)
O(1w)-H(1wA)...N(7a)	0.935	1.97(1)	2.866(1)	160.8(1)
O(1w)-H(1wA)...N(8a)	0.935	2.67(1)	3.301(1)	125.4(1)

**Figure 4.** View along the crystallographic *b* axis of the intermolecular interactions between  $[\text{ReCl}_4(\text{bpym})]$  complexes and between  $[\text{ReCl}_4(\text{bpym})]$  complexes and MeCN molecules in **1** (left); View along the crystallographic *a* axis of the intermolecular interactions between  $[\text{ReCl}_4(\text{bpym})]$  complexes and  $\text{CH}_3\text{COOH}$  and  $\text{H}_2\text{O}$  molecules in **2** (right).

In **2**, there are  $\pi \cdots \text{Cl}$  contacts involving bipyrimidine rings and chloride anions, which are of approximately 3.283(1) Å. There are also weak C-H...Cl interactions, which implicate the methyl group of the  $\text{CH}_3\text{COOH}$  molecules and chloride anions of the  $[\text{ReCl}_4(\text{bpym})]$  complexes [C(18)...Cl(5d) distance of ca. 3.617 Å; (d) =  $x + 1, -y + 3/2, z - 1/2$ ]. These last intermolecular interactions contribute to stabilizing the crystal structure in compound **2** (Figure 4).

### 2.3. Hirshfeld Surface Analysis

Hirshfeld surfaces of the neutral  $[\text{ReCl}_4(\text{bpym})]$  complex in compounds **1** and **2** were calculated. The close intermolecular interactions were analyzed through the CrystalExplorer program and compared with those of the non-solvated  $[\text{ReCl}_4(\text{bpym})]$  complex [35–37]. CrystalExplorer calculates a series of surfaces which allow users to obtain both a qualitative and quantitative visualization of the main intermolecular interactions. In this case, taking place in **1** and **2**, the shorter contacts are shown using a red color [38,39]. This is performed by mapping the distances from the surface to the nearest atom outside ( $d_e$ ) and inside ( $d_i$ ) of each surface and, at the same time, assuming a normalized contact distance ( $d_{\text{norm}}$ ) that considers some limitations generated by the atomic radii [35–37]. The Hirshfeld surfaces for these bpym-based compounds are given in Figures 5–7 and Figures S1–S3 (Supplementary Materials). According to their fingerprint plots, both **1** and **2** show a very similar percentage regarding the intermolecular Cl...Cl contacts between adjacent  $[\text{ReCl}_4(\text{bpym})]$  complexes (ca. 6.4% for **1** and ca. 6.3% for **2**), which is consistent with the similar framework based on halogen bonds that both compounds exhibit (Figure 8). The Cl...H contacts, primarily connecting chloride anions and C-H groups of neighboring  $[\text{ReCl}_4(\text{bpym})]$  complexes in **1** and **2**, and the methyl groups of  $\text{CH}_3\text{COOH}$  molecules in the case of **2**, are the main interactions observed on the Hirshfeld surfaces for both compounds, which cover ca. 34.9% for **1** and ca. 39.2% for **2** on their respective fingerprint plots (Figures 5 and 6). Finally, further N...H contacts involving solvent molecules, mainly MeCN (in **1**) and  $\text{H}_2\text{O}$  (in **2**), and N atoms and C-H groups of adjacent bipyrimidine rings, are approximately 11.6% and 9.7% of the complete fingerprint plot of **1** and **2**, respectively (Figures 5 and 6). In Figure 6, a small asymmetric region close to

the  $d_i$  values (1.2–1.4) is observed, which could be the result of some structural disorder, as previously reported [40–43]. The fingerprint plots for the non-solvated  $[\text{ReCl}_4(\text{bpym})]$  complex show a similar percentage for the intermolecular  $\text{Cl} \cdots \text{Cl}$  contacts (ca. 6.0%) and a higher contribution of the  $\text{Cl} \cdots \text{H}$  interactions (ca. 43.5%), involving chloride anions and C-H groups of bipyrimidine rings of adjacent  $[\text{ReCl}_4(\text{bpym})]$  complexes (Figures 7 and S3).

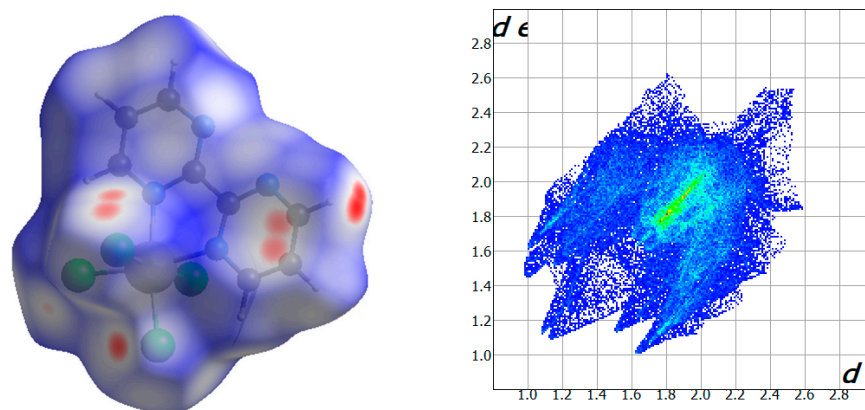


**Figure 5.** Hirshfeld surface mapped through  $d_{\text{norm}}$  function for **1** (left); Full fingerprint plot for the dinuclear Re(IV) compound **1** (right).

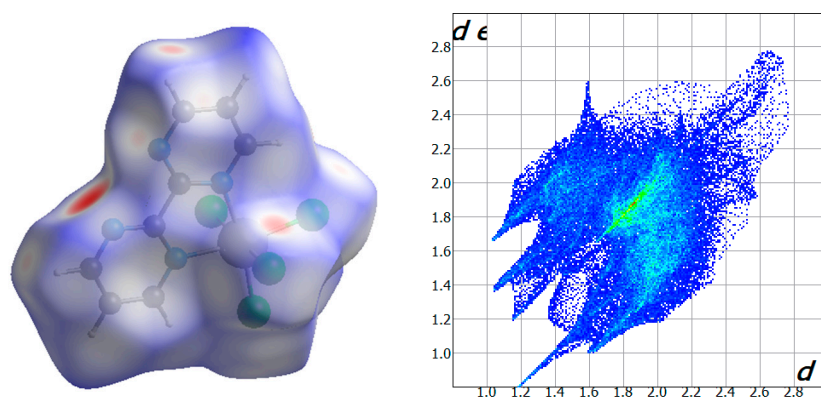


**Figure 6.** Hirshfeld surface mapped through  $d_{\text{norm}}$  function for **2** (left); Full fingerprint plot for the dinuclear Re(IV) compound **2** (right).

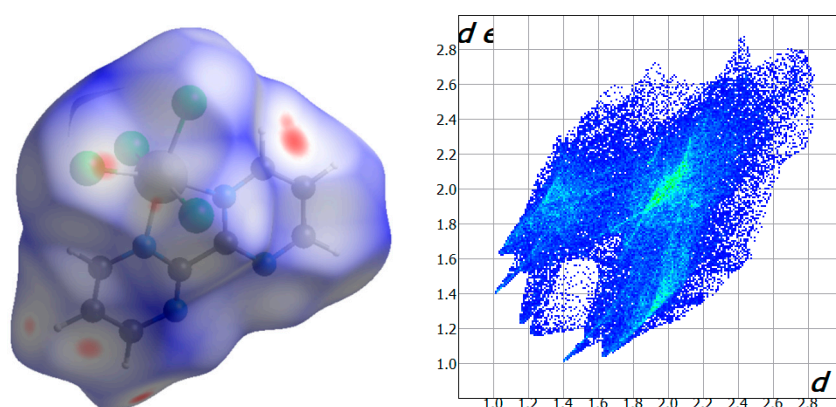


**Figure 7.** Hirshfeld surface mapped through  $d_{\text{norm}}$  function for the non-solvated  $[\text{ReCl}_4(\text{bpym})]$  complex (left); Full fingerprint plot for the non-solvated  $[\text{ReCl}_4(\text{bpym})]$  complex (right).

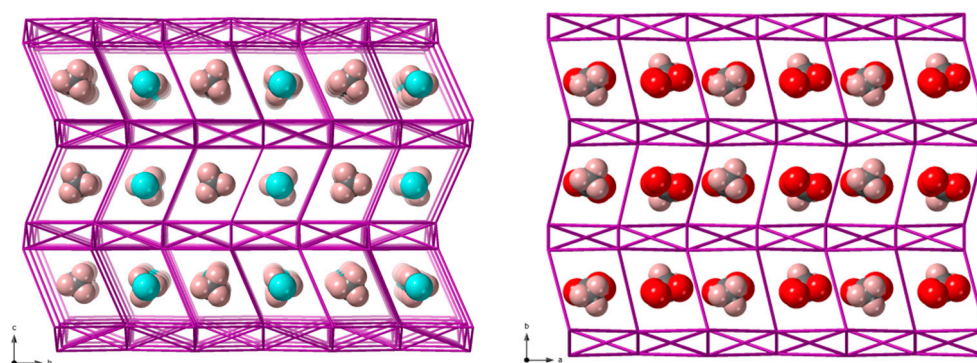


**Figure 8.** View along the crystallographic *a* axis of the grid formed by  $[\text{ReCl}_4(\text{bpym})]$  complexes connected through intermolecular  $\text{Cl} \cdots \text{Cl}$  interactions acting as host of MeCN molecules in **1** (left); View along the crystallographic *c* axis of the grid formed by  $[\text{ReCl}_4(\text{bpym})]$  complexes connected through intermolecular  $\text{Cl} \cdots \text{Cl}$  interactions acting as host of  $\text{CH}_3\text{COOH}$  and  $\text{H}_2\text{O}$  molecules in **2** (right).

#### 2.4. Magnetic Properties

Dc magnetic susceptibility measurements were performed on microcrystalline samples of **1** and **2** in the 2–300 K temperature range and under an external magnetic field of 0.5 T. The resulting  $\chi_M T$  versus  $T$  plots ( $\chi_M$  being the molar magnetic susceptibility per mononuclear Re(IV) complex) for compounds **1** and **2** are shown in Figure 9. At 300 K, the  $\chi_M T$  values are ca. 1.57 (**1**) and ca. 1.54  $\text{cm}^3 \text{mol}^{-1} \text{K}$  (**2**). These are very close to those previously published for magnetically isolated complexes based on Re(IV) ion ( $5d^3$  ion with  $S = 3/2$ ) [7]. Upon cooling, the curve that the  $\chi_M T$  values draw for **1** follows the Curie law, with decreasing temperature to approximately 100 K before they decrease reaching minimum values of approximately 0.17  $\text{cm}^3 \text{mol}^{-1} \text{K}$  at 2.0 K (Figure 9). In the case of **2**, the  $\chi_M T$  values decrease gradually with the decreasing temperature, and more abruptly at approximately 50 K, reaching a minimum value of 0.49  $\text{cm}^3 \text{mol}^{-1} \text{K}$  at 2.0 K (Figure 9). The decrease in the  $\chi_M T$  value observed for both **1** and **2** is assignable to antiferromagnetic interactions as well as zero-field splitting (ZFS) effects [44–46]. No maximum of the magnetic susceptibility is observed for either compound, as shown in their respective  $\chi_M$  vs.  $T$  plots (insets in Figure 9). Room temperature magnetization values for **1** and **2** are ca. 1.55 and ca. 1.58  $\mu_B$ , respectively. They are very close to those values of earlier published mononuclear Re(IV) complexes [7].

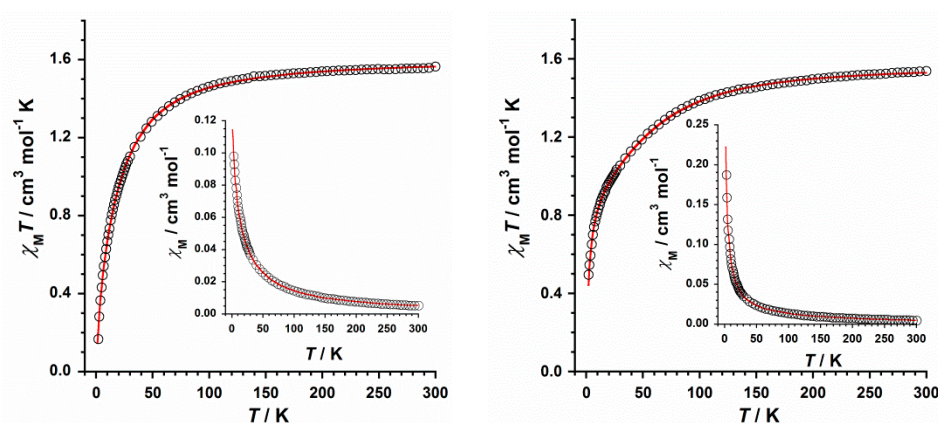


**Figure 9.** Thermal variation of the  $\chi_M T$  product for compounds **1** (left) and **2** (right). The solid red line represents the theoretical fit of the experimental data and the inset shows the  $\chi_M$  versus  $T$  plot.

As indicated in the description of the crystal structure of **1** and **2**, both compounds exhibit short  $\text{Cl} \cdots \text{Cl}$  contacts between the paramagnetic  $[\text{ReCl}_4(\text{bpym})]$  complexes in their crystal lattices (Figure 3). Hence, these relatively important through-space interactions

between Re(IV) ions precludes the occurrence of SIM behavior [44,45]. Additionally, the presence of solvent molecules drastically changes the magnetic properties, given that the unsolvated [ReCl<sub>4</sub>(bpym)] complex exhibits magnetic ordering through spin-canting. As previously reported [7,28], this is a magnetic behavior observed in neither **1** nor in **2**.

$$\hat{H} = D \left[ (\hat{S}_Z)^2 - S(S+1)/3 \right] + g\beta H \hat{S} \quad (1)$$

$$\begin{aligned} \chi_M &= \frac{\chi_{//} + 2\chi_{\perp}}{3} \\ \chi_{//} &= \frac{N\beta^2 g_{//}^2}{4k(T-\theta)} \frac{1+9\exp(-2D/kT)}{1+\exp(-2D/kT)} \\ \chi_{\perp} &= \frac{N\beta^2 g_{\perp}^2}{k(T-\theta)} \frac{1+(3kT/4D)[1-\exp(-2D/kT)]}{1+\exp(-2D/kT)} \end{aligned} \quad (2)$$

To analyze the magnetic behavior of **1** and **2**, we employed the Hamiltonian of Equation (1) and its derived theoretical expression for the magnetic susceptibility of Equation (2), by including a  $\theta$  term to account for the observed intermolecular interactions, where  $\hat{S}_Z$  is the easy-axis spin operator,  $H$  is the applied field,  $\beta$  is the Bohr magneton, the  $g$  parameter is the Landé factor and  $D$  is the zero-field splitting (ZFS) for the Re(IV) ion [7]. As previously reported, the zero-field splitting values for Re(IV) (a 5d<sup>3</sup> ion) are very large in a distorted octahedral environment because of the high value of the spin-orbit coupling constant ( $\lambda$  ca. 1000 cm<sup>-1</sup> in the free ion). In fact, for a six-coordinate Re(IV) ion, as in compounds **1** and **2**, the first excited term which arises from the <sup>4</sup>F free-ion ground term is <sup>4</sup>T<sub>2g</sub>. Under a tetragonal distortion, this excited state is split into orbital singlet <sup>4</sup>B<sub>2</sub> and orbital doublet <sup>4</sup>E at energies  $\Delta_{\parallel}$  and  $\Delta_{\perp}$ , respectively [7]. Under this pattern, the interaction of these two excited terms, with the quartet ground spin state, leads to two Kramers doublets,  $|\pm 3/2\rangle$  and  $|\pm 1/2\rangle$ , which are separated by an energy gap of  $|2D|$ ; that is, the zero-field splitting resulting from the combined action of second-order spin-orbit interaction and the tetragonal crystal field.

Thus, the first term in Equation (1) corresponds to the ZFS and the second term to the Zeeman effect. Additionally, we have assumed that  $g_{\parallel} = g_{\perp} = g$  for complexes **1** and **2**. The best least-squares fit gave the parameters  $D = 31.9$  cm<sup>-1</sup>,  $g = 1.86$ ,  $\theta = -5.3$  K and  $R = 2.94 \times 10^{-5}$  for **1** and  $D = 35.8$  cm<sup>-1</sup>,  $g = 1.83$ ,  $\theta = -8.8$  K and  $R = 4.52 \times 10^{-5}$  for **2** ( $R$  being the agreement factor defined as  $\sum_i [(\chi_M T)_i^{\text{obs}} - (\chi_M T)_i^{\text{calcd}}]^2 / [(\chi_M T)_i^{\text{obs}}]^2$ ). As shown in Figure 9, the calculated curves (solid red lines) reproduce the experimental magnetic data in the whole temperature range quite well. The  $D$  and  $g$  values calculated for **1** and **2** are in agreement with those earlier reported for mononuclear Re(IV) complexes [7,8]. The sign and magnitude of the  $\theta$  values corroborate the presence of relatively strong antiferromagnetic exchanges between the Re(IV) ions connected through intermolecular Cl...Cl and  $\pi$ ...Cl pathways (Figure 3), with the shorter interactions being in **2** [ca. 3.6 Å (in **1**) versus ca. 3.3 Å (in **2**)]. According to the literature, these are considered halogen bonds and result in stronger antiferromagnetic exchange [47,48].

### 3. Experimental Section

#### 3.1. Materials

All manipulations were performed under aerobic conditions, using all solvents and chemicals as received. The Re(IV) precursors, [ReCl<sub>4</sub>(bpym)] and (NBu<sub>4</sub>)<sub>2</sub>[ReCl<sub>4</sub>(ox)], were prepared following their respective literature procedures [26,49].

#### 3.2. Synthesis of the Complexes

##### 3.2.1. Synthesis and Crystallization of [ReCl<sub>4</sub>(bpym)]·MeCN (**1**)

The preparation of **1** consisted of dissolving [ReCl<sub>4</sub>(bpym)] (0.05 mmol, 24.3 mg) in 2 mL of a N,N-dimethylformamide-acetonitrile (1:1, v/v) mixture, followed by a slow diffusion in isopropanol at room temperature. Brown crystals of **1** were thus obtained in a few days and were suitable for single-crystal X-ray diffraction studies. Yield: ca. 75%. Anal. Calcd. for C<sub>18</sub>H<sub>15</sub>N<sub>9</sub>Cl<sub>8</sub>Re<sub>2</sub> (**1**): C, 21.3; H, 1.5; N, 12.4. Found: C, 20.9; H, 1.1; N,

12.3. SEM-EDX: a molar ratio of 1:4 for Re/Cl was found for **1** (Figure S4). IR (KBr pellet) peaks are observed at 3100 (m), 3067 (s), 2245 (m), 1578 (vs), 1541 (m), 1453 (w), 1407 (vs), 1269 (w), 1213 (m), 1113 (m), 1021 (s), 987 (w), 818 (m), 747 (s), 693 (m), 665 (s), 490 (w), 440 (w)  $\text{cm}^{-1}$  (Figure S5).

### 3.2.2. Synthesis and Crystallization of $[\text{ReCl}_4(\text{bpym})]\cdot\text{CH}_3\text{COOH}\cdot\text{H}_2\text{O}$ (**2**)

The preparation of **2** consisted of the ligand substitution of the previously reported  $(\text{NBu}_4)_2[\text{ReCl}_4(\text{ox})]$  complex.  $(\text{NBu}_4)_2[\text{ReCl}_4(\text{ox})]$  (0.12 mmol, 110 mg) and 2,2'-bipyrimidine (0.25 mmol, 39.5 mg) were mixed in glacial acetic acid (4.0 mL). The mixture was heated to 100 °C and stirred for 4 h. The resulting solution was filtered while hot and left to evaporate at room temperature. Dark orange crystals of **2** were grown in less than 1 week and were suitable for X-ray diffraction data collection. Yield: ca. 60%. Anal. Calcd for  $\text{C}_{18}\text{H}_{18}\text{N}_8\text{O}_3\text{Cl}_8\text{Re}_2$  (**2**): C, 20.6; H, 1.7; N, 10.7. Found: C, 21.0; H, 2.0; N, 10.6. SEM-EDX: a molar ratio of 1:4 for Re/Cl was found for **2** (Figure S6). IR (KBr pellet) peaks are observed at 3424 (br), 3091 (m), 3066 (m), 1711 (m), 1579 (vs), 1547 (m), 1452 (w), 1436 (w), 1406 (vs), 1303 (w), 1258 (m), 1211 (w), 1109 (m), 1024 (s), 989 (w), 877 (w), 819 (m), 748 (s), 695 (m), 669 (m), 617 (w), 515 (w)  $\text{cm}^{-1}$  (Figure S7).

### 3.3. X-ray Data Collection and Structure Refinement

X-ray diffraction data collection on single crystals of dimensions  $0.28 \times 0.21 \times 0.21$  (**1**) and  $0.17 \times 0.16 \times 0.06$   $\text{mm}^3$  (**2**) was carried out on a Bruker D8 Venture diffractometer with PHOTON II detector, using monochromatized Mo- $\text{K}\alpha$  radiation ( $\lambda = 0.71073$  Å). Crystal parameters and refinement results for **1** and **2** are summarized in Table 1. The structures were solved by standard direct methods and subsequently completed by Fourier recycling using the SHELXTL [50] software packages and refined by the full-matrix least-squares refinements based on  $F^2$  with all observed reflections. The final graphical manipulations were performed with the DIAMOND [51] and CRYSTALMAKER [52] programs. Crystallographic data were deposited in the Cambridge Structural Data Centre (CCDC) with numbers 2233243 and 2233244 for **1** and **2**, respectively.

### 3.4. Physical Measurements

Elemental analyses (C, H, N) were performed in an Elemental Analyzer CE Instruments CHNS1100 and the molar ratio between heavier elements was found by means of a Philips XL-30 scanning electron microscope (SEM-EDX), equipped with system of X-ray microanalysis, in the Central Service for the Support to Experimental Research (SCSIE) at the University of Valencia. Infrared spectra (IR) of **1** and **2** were recorded with a PerkinElmer Spectrum 65 FT-IR spectrometer in the  $4000\text{--}400$   $\text{cm}^{-1}$  region. Variable-temperature, solid-state dc magnetic susceptibility data were collected on a Quantum Design MPMS-XL SQUID magnetometer equipped with a 5 T dc magnet. To keep the samples of compounds **1** and **2** both immobilized and well isolated from the moisture of the air at all times, the organic compound eicosene was employed. Experimental magnetic data were corrected for the diamagnetic contributions of both the sample holder and the eicosene. The diamagnetic contribution of the involved atoms was corrected using Pascal's constants [53].

## 4. Conclusions

In summary, the synthesis, crystal structure and magnetic properties of two novel solvated Re(IV) complexes based on the 2,2'-bipyrimidine ligand, with formula  $[\text{ReCl}_4(\text{bpym})]\cdot\text{MeCN}$  (**1**) and  $[\text{ReCl}_4(\text{bpym})]\cdot\text{CH}_3\text{COOH}\cdot\text{H}_2\text{O}$  (**2**), have been reported. In the crystal structures of **1** and **2**, there are intermolecular halogen...halogen and  $\pi$ ...halogen-type interactions present and, in compound **2** only, there exist O-H...O and O-H...N hydrogen bonds. Having taken into account the presence of Cl...Cl interactions and halogen bonds, both compounds exhibit corrugated, reticular crystal frameworks, which host the solvent molecules. The investigation of the magnetic properties of **1** and **2** through dc magnetic susceptibility measurements reveals a similar magnetic behavior,

since both compounds display antiferromagnetic exchange couplings between neighboring Re(IV) ions. The magnetic properties can be drastically modified by the presence of solvent molecules, given that the non-solvated [ReCl<sub>4</sub>(bpym)] complex exhibits a very different magnetic behavior (that is, magnetic ordering) through spin-canting, as previously reported. As such, by changing suitable solvents, it is possible to tune the magnetic properties in this type of molecular-based Re(IV) compounds. Further work based on other halides of the Re(IV) ion and other solvents is in progress.

**Supplementary Materials:** The following supporting information can be downloaded at: <https://www.mdpi.com/article/10.3390/inorganics11020078/s1>, Figure S1. Fingerprint plots for the [ReCl<sub>4</sub>(bpym)] complex in **1** highlighting the region assigned to the N···H interactions (left) and to the Cl···H interactions (right). Figure S2. Fingerprint plots for the [ReCl<sub>4</sub>(bpym)] complex in **2** highlighting the region assigned to the O···H interactions (left) and to the Cl···H interactions (right). Figure S3. Fingerprint plots for the non-solvated [ReCl<sub>4</sub>(bpym)] complex highlighting the region assigned to the N···H interactions (left) and to the Cl···H interactions (right). Figure S4. SEM-EDX spectrum for compound **1**. Figure S5. Infrared spectrum (FT-IR) for compound **1**. Figure S6. SEM-EDX spectrum for compound **2**. Figure S7. Infrared spectrum (FT-IR) for compound **2**.

**Author Contributions:** Conceptualization, J.M.-L.; funding acquisition, J.M.-L.; methodology, A.S.-P., M.O.-A., N.M. and J.M.-L.; investigation, A.S.-P., M.O.-A., N.M. and J.M.-L.; formal analysis, A.S.-P., M.O.-A., N.M. and J.M.-L.; writing—original draft preparation, J.M.-L.; writing—review and editing, J.M.-L. All authors have read and agreed to the published version of the manuscript.

**Funding:** This research was funded by Spanish Ministry of Science and Innovation (Grant numbers PID2019-109735GB-I00 and CEX2019-000919-M (Excellence Unit “María de Maeztu”).

**Institutional Review Board Statement:** Not applicable.

**Informed Consent Statement:** Not applicable.

**Data Availability Statement:** The raw data that support the findings of this study are available from the corresponding author upon reasonable request.

**Acknowledgments:** A.S.-P. and M.O.-A. thank the Spanish “FPU fellowships” and “FPI fellowships” programs, respectively.

**Conflicts of Interest:** The authors declare no conflict of interest.

## References

1. Price, C.P.; Glick, G.D.; Matzger, A.J. Dissecting the Behavior of a Promiscuous Solvate Former. *Angew. Chem. Int. Ed.* **2006**, *45*, 2062–2066. [[CrossRef](#)] [[PubMed](#)]
2. Shan, N.; Zaworotko, M.J. The role of cocrystals in pharmaceutical science. *Drug Discov.* **2008**, *13*, 440–446. [[CrossRef](#)] [[PubMed](#)]
3. Cruz-Cabeza, A.J.; Reutzel-Edens, S.M.; Bernstein, J. Facts and fictions about polymorphism. *Chem. Soc. Rev.* **2015**, *44*, 8619–8635. [[CrossRef](#)] [[PubMed](#)]
4. Takiyeddin, K.; Khimiyak, Y.Z.; Fábíán, L. Prediction of Hydrate and Solvate Formation Using Statistical Models. *Cryst. Growth Des.* **2016**, *16*, 70–81. [[CrossRef](#)]
5. Braga, D.; Casali, L.; Grepioni, F. The Relevance of Crystal Forms in the Pharmaceutical Field: Sword of Damocles or Innovation Tools? *Int. J. Mol. Sci.* **2022**, *23*, 9013. [[CrossRef](#)]
6. Martínez-Lillo, J.; Armentano, D.; Mastropietro, T.F.; Julve, M.; Faus, J.; De Munno, G. Self-Assembled One- and Two-Dimensional Networks Based on NH<sub>2</sub>Me<sub>2</sub>[ReX<sub>5</sub>(DMF)] (X = Cl and Br) Species: Polymorphism and Supramolecular Isomerism in Re(IV) Compounds. *Cryst. Growth Des.* **2011**, *11*, 1733–1741. [[CrossRef](#)]
7. Martínez-Lillo, J.; Faus, J.; Lloret, F.; Julve, J. Towards multifunctional magnetic systems through molecular-programmed self assembly of Re(IV) metalloligands. *Coord. Chem. Rev.* **2015**, *289–290*, 215–237. [[CrossRef](#)]
8. Woodall, C.H.; Craig, G.A.; Prescimone, A.; Misek, M.; Cano, J.; Faus, J.; Probert, M.R.; Parsons, S.; Moggach, S.; Martínez-Lillo, J.; et al. Pressure induced enhancement of the magnetic ordering temperature in rhenium(IV) monomers. *Nat. Commun.* **2016**, *7*, 13870. [[CrossRef](#)]
9. González, R.; Chiozzzone, R.; Kremer, C.; Guerra, F.; De Munno, G.; Lloret, F.; Julve, M.; Faus, J. Magnetic Studies on Hexahalorhenate(IV) Salts of Ferrocenium Cations [Fe(C<sub>5</sub>R<sub>5</sub>)<sub>2</sub>]<sub>2</sub>[ReX<sub>6</sub>] (R = H, CH<sub>3</sub>; X = Cl, Br, I). *Inorg. Chem.* **2004**, *43*, 3013–3019. [[CrossRef](#)]
10. Nelson, C.M.; Boyd, G.E.; Smith, W.T. Magnetochemistry of Technetium and Rhenium. *J. Am. Chem. Soc.* **1954**, *76*, 348–352. [[CrossRef](#)]

11. Figgis, B.N.; Lewis, J.; Mabbs, F.E. The Magnetic Properties of Some  $d^3$ -Complexes. *J. Chem. Soc.* **1961**, 3138–3145. [[CrossRef](#)]
12. Busey, R.; Sonder, E. Magnetic Susceptibility of Potassium Hexachlororhenate (IV) and Potassium Hexabromorhenate (IV) from 5° to 300 °K. *J. Chem. Phys.* **1962**, *36*, 93–97. [[CrossRef](#)]
13. Rouschias, G.; Wilkinson, G. The chemistry of rhenium–nitrile complexes. *J. Chem. Soc. A* **1968**, 489–496. [[CrossRef](#)]
14. Mroziński, J. Magnetic properties of methylammonium hexachlororhenate (4) salts in the range 1.5–300 K. *Bull. Pol. Acad. Sci. Chem.* **1978**, *26*, 789–798.
15. Mroziński, J. Low temperature magnetic properties of some methylammonium hexabromorhenate (4) salts. *Bull. Pol. Acad. Sci. Chem.* **1980**, *28*, 559–567.
16. Reynolds, P.A.; Moubaraki, B.; Murray, K.S.; Cable, J.W.; Engelhardt, L.M.; Figgis, B.N. Metamagnetism in tetrachlorobis(N-phenylacetamidine)rhenium(IV). *J. Chem. Soc. Dalton Trans.* **1997**, 263–268. [[CrossRef](#)]
17. Małecka, J.; Jäger, L.; Wagner, C.; Mroziński, J. Preparation, crystal structure and properties of  $(\text{Ph}_4\text{P})_2\text{ReCl}_6 \cdot 2\text{CH}_3\text{CN}$ . *Pol. J. Chem.* **1998**, *72*, 1879–1885.
18. Reynolds, P.A.; Figgis, B.N.; Martín y Marero, D.J. Magnetic structure and covalence in tetrachlorobis(N-phenylacetamidinato)rhenium(IV) by neutron diffraction. *J. Chem. Soc. Dalton Trans.* **1999**, 945–950. [[CrossRef](#)]
19. Thornton, P. 13 Manganese, technetium and rhenium. *Annu. Rep. Prog. Chem. Sect. A Inorg. Chem.* **2000**, *96*, 215–228. [[CrossRef](#)]
20. Coronado, E.; Day, P. Magnetic Molecular Conductors. *Chem. Rev.* **2004**, *104*, 5419–5448. [[CrossRef](#)]
21. Feng, X.; Liu, J.-L.; Pedersen, K.S.; Nehrkorn, J.; Schnegg, A.; Holldack, K.; Bendix, J.; Sigrist, M.; Mutka, H.; Samohvalov, D.; et al. Multifaceted magnetization dynamics in the mononuclear complex  $[\text{Re}^{\text{IV}}\text{Cl}_4(\text{CN})_2]^{2-}$ . *Chem. Commun.* **2016**, *52*, 12905–12908. [[CrossRef](#)] [[PubMed](#)]
22. Pedersen, K.S.; Sigrist, M.; Sørensen, M.A.; Barra, A.-L.; Weyhermüller, T.; Piligkos, S.; Thuesen, C.A.; Vinum, M.G.; Mutka, H.; Weihe, H.; et al.  $[\text{ReF}_6]^{2-}$ : A Robust Module for the Design of Molecule-Based Magnetic Materials. *Angew. Chem. Int. Ed.* **2014**, *53*, 1351–1354. [[CrossRef](#)] [[PubMed](#)]
23. González, R.; Chiozzzone, R.; Kremer, C.; De Munno, G.; Nicolò, F.; Lloret, F.; Julve, M.; Faus, J. Magnetic Studies on Hexaiodorhenate(IV) Salts of Univalent Cations. Spin Canting and Magnetic Ordering in  $\text{K}_2[\text{ReI}_6]$  with  $T_c = 24$  K. *Inorg. Chem.* **2003**, *42*, 2512–2518. [[CrossRef](#)] [[PubMed](#)]
24. Martínez-Lillo, J.; Kong, J.; Barros, W.P.; Faus, J.; Julve, M.; Brechin, E.K. Metamagnetic behaviour in a new Cu(II)Re(IV) chain based on the hexachlororhenate(IV) anion. *Chem. Commun.* **2014**, *50*, 5840–5842. [[CrossRef](#)]
25. Louis-Jean, J.; Balasekaran, S.M.; Lawler, K.V.; Sanchis-Perucho, A.; Martínez-Lillo, J.; Smith, D.; Forster, P.M.; Salamat, A.; Poineau, F. Coexistence of metamagnetism and slow relaxation of magnetization in ammonium hexafluoridorhenate. *RSC Adv.* **2021**, *11*, 6353–6360. [[CrossRef](#)]
26. Chiozzzone, R.; González, R.; Kremer, C.; Cerdá, M.F.; Armentano, D.; De Munno, G.; Martínez-Lillo, J.; Faus, J. A novel series of rhenium-bipyrimidine complexes: Synthesis, crystal structure and electrochemical properties. *Dalton Trans.* **2007**, *6*, 653–660. [[CrossRef](#)]
27. Martínez-Lillo, J.; Mastropietro, T.F.; Lappano, R.; Madeo, A.; Alberto, M.E.; Russo, N.; Maggiolini, M.; De Munno, G. Rhenium(IV) compounds inducing apoptosis in cancer cells. *Chem. Commun.* **2011**, *47*, 5283–5285. [[CrossRef](#)]
28. Martínez-Lillo, J.; Lloret, F.; Julve, M.; Faus, J. Spin canting in Re(IV) complexes: Magnetic properties of  $[\text{ReX}_4(\text{bpym})]$  ( $X = \text{Cl}$  and  $\text{Br}$ ;  $\text{bpym} = 2,2'$ -bipyrimidine). *J. Coord. Chem.* **2008**, *62*, 92–99. [[CrossRef](#)]
29. Martínez-Lillo, J.; Armentano, D.; De Munno, G.; Cano, J.; Lloret, F.; Julve, M.; Faus, J. First Magnetostructural Study on a Heterodinuclear 2,2'-Bipyrimidine-Bridged Complex. *Inorg. Chem.* **2011**, *50*, 12405–12407. [[CrossRef](#)]
30. Martínez-Lillo, J.; Armentano, D.; Fortea-Pérez, F.R.; Stiriba, S.E.; De Munno, G.; Lloret, F.; Julve, M.; Faus, J. A Chiral, Photoluminescent, and Spin-Canted  $[\text{Cu}^{\text{I}}\text{Re}^{\text{IV}}_2]_n$  Branched Chain. *Inorg. Chem.* **2015**, *54*, 4594–4596. [[CrossRef](#)]
31. Armentano, D.; Sanchis-Perucho, A.; Rojas-Dotti, C.; Martínez-Lillo, J. Halogen···halogen interactions in the self-assembly of one-dimensional 2,2'-bipyrimidine-based  $\text{Cu}^{\text{II}}\text{Re}^{\text{IV}}$  systems. *CrystEngComm* **2018**, *20*, 4575–4581. [[CrossRef](#)]
32. Martínez-Lillo, J.; Armentano, D.; De Munno, G.; Faus, J. Magneto-structural study on a series of rhenium(IV) complexes containing biimH<sub>2</sub>, pyim and bipy ligands. *Polyhedron* **2008**, *27*, 1447–1454. [[CrossRef](#)]
33. Roy, N.; Sen, U.; Moharana, P.; Babu, L.T.; Kar, B.; Vardhan, S.; Sahoo, S.K.; Bose, B.; Paira, P. 2,2'-Bipyrimidine-based luminescent Ru(II)/Ir(III)–arene monometallic and homo- and hetero-bimetallic complexes for therapy against MDA-MB-468 and caco-2 cells. *Dalton Trans.* **2021**, *50*, 11725–11729. [[CrossRef](#)]
34. Yao, S.-Y.; Ou, Y.-L.; Ye, B.-H. Asymmetric Synthesis of Enantiomerically Pure Mono- and Binuclear Bis(cyclometalated) Iridium(III) Complexes. *Inorg. Chem.* **2016**, *55*, 6018–6026. [[CrossRef](#)]
35. Turner, M.J.; McKinnon, J.J.; Wolff, S.K.; Grimwood, D.J.; Spackman, P.R.; Jayatilaka, D.; Spackman, M.A. *CrystalExplorer 17*; University of Western Australia: Perth, Australia, 2017.
36. McKinnon, J.J.; Jayatilaka, D.; Spackman, M.A. Towards quantitative analysis of intermolecular interactions with Hirshfeld surfaces. *Chem. Commun.* **2007**, 3814–3816. [[CrossRef](#)]
37. Spackman, M.A.; Jayatilaka, D. Hirshfeld surface analysis. *CrystEngComm* **2009**, *11*, 19–32. [[CrossRef](#)]
38. Spackman, P.R.; Turner, M.J.; McKinnon, J.J.; Wolff, S.K.; Grimwood, D.J.; Jayatilaka, D.; Spackman, M.A. CrystalExplorer: A program for Hirshfeld surface analysis, visualization and quantitative analysis of molecular crystals. *J. Appl. Cryst.* **2021**, *54*, 1006–1011. [[CrossRef](#)]

39. Li, S.; Bu, R.; Gou, R.-J.; Zhang, C. Hirshfeld Surface Method and Its Application in Energetic Crystals. *Cryst. Growth Des.* **2021**, *21*, 6619–6634. [[CrossRef](#)]
40. Martin, A.D.; Britton, J.; Easun, T.L.; Blake, A.J.; Lewis, W.; Schröder, M. Hirshfeld Surface Investigation of Structure-Directing Interactions within Dipicolinic Acid Derivatives. *Cryst. Growth Des.* **2015**, *15*, 1697–1706. [[CrossRef](#)]
41. Orts-Arroyo, M.; Castro, I.; Lloret, F.; Martínez-Lillo, J. Molecular Self-Assembly in a Family of Oxo-Bridged Dinuclear Ruthenium(IV) Systems. *Cryst. Growth Des.* **2020**, *20*, 2044–2056. [[CrossRef](#)]
42. Sanchis-Perucho, A.; Orts-Arroyo, M.; Camús-Hernández, J.; Rojas-Dotti, C.; Escrivà, E.; Lloret, F.; Martínez-Lillo, J. Hexahalorhenate(IV) salts of protonated ciprofloxacin: Antibiotic-based single-ion magnets. *CrystEngComm* **2021**, *23*, 8579–8587. [[CrossRef](#)]
43. Sanchis-Perucho, A.; Orts-Arroyo, M.; Castro, I.; Lloret, F.; Martínez-Lillo, J. Crystal polymorphism in 2,2'-bipyrimidine-based iridium(III) complexes. *J. Coord. Chem.* **2022**, *75*, 2495–2507. [[CrossRef](#)]
44. McAdams, S.G.; Ariciu, A.M.; Kostopoulos, A.K.; Walsh, J.P.S.; Tuna, F. Molecular single-ion magnets based on lanthanides and actinides: Design considerations and new advances in the context of quantum technologies. *Coord. Chem. Rev.* **2017**, *346*, 216–239. [[CrossRef](#)]
45. Zabala-Lekuona, A.; Seco, J.M.; Colacio, E. Single-Molecule Magnets: From Mn12-ac to dysprosium metallocenes, a travel in time. *Coord. Chem. Rev.* **2021**, *441*, 213984. [[CrossRef](#)]
46. Uysal, Ş. The Synthesis and Characterization of Star Shaped Metal Complexes of Triazine Cored Schiff Bases: Their Thermal Decompositions and Magnetic Moment Values. *J. Inorg. Organomet. Pol. Mat.* **2011**, *21*, 291–296. [[CrossRef](#)]
47. Batsanov, S.S. Van der Waals Radii of Elements. *Inorg. Mater.* **2001**, *37*, 871–885. [[CrossRef](#)]
48. Álvarez, S. A cartography of the van der Waals territories. *Dalton Trans.* **2013**, *42*, 8617–8636. [[CrossRef](#)]
49. Chiozzone, R.; González, R.; Kremer, C.; De Munno, G.; Cano, J.; Lloret, F.; Julve, M.; Faus, J. Synthesis, Crystal Structure, and Magnetic Properties of Tetraphenylarsonium Tetrachloro(oxalato)rhenate(IV) and Bis(2,2'-bipyridine)tetrachloro( $\mu$ -oxalato)copper(II)rhenium(IV). *Inorg. Chem.* **1999**, *38*, 4745–4752. [[CrossRef](#)]
50. *SHELXTL-2013/4*; Bruker Analytical X-ray Instruments. Bruker: Madison, WI, USA, 2013.
51. *Diamond*, version 4.5.0; Crystal Impact GbR: Bonn, Germany, 2018.
52. *CrystalMaker*, version 8.5.1; CrystalMaker Software Ltd.: Oxford, UK.
53. Bain, G.A.; Berry, J.F. Diamagnetic Corrections and Pascal's Constants. *J. Chem. Educ.* **2008**, *85*, 532–536. [[CrossRef](#)]

**Disclaimer/Publisher's Note:** The statements, opinions and data contained in all publications are solely those of the individual author(s) and contributor(s) and not of MDPI and/or the editor(s). MDPI and/or the editor(s) disclaim responsibility for any injury to people or property resulting from any ideas, methods, instructions or products referred to in the content.